PAPER

Dither Signal Design for PAPR Reduction in OFDM-IM over a Rayleigh Fading Channel*

Kee-Hoon KIM[†a)], ***Nonmember***

SUMMARY Orthogonal frequency division multiplexing with index modulation (OFDM-IM) is a novel scheme where the information bits are conveyed through the subcarrier activation pattern (SAP) and the symbols on the active subcarriers. Specifically, the subcarriers are partitioned into many subblocks and the subcarriers in each subblock can have two states, active or idle. Unfortunately, OFDM-IM inherits the high peak-to-average power ratio (PAPR) problem from the classical OFDM. The OFDM-IM signal with high PAPR induces in-band distortion and out-of-band radiation when it passes through high power amplifier (HPA). Recently, there are attempts to reduce PAPR by exploiting the unique structure of OFDM-IM, which is adding dither signals in the idle subcarriers. The most recent work dealing with the dither signals is using dithers signals with various amplitude constraints according to the characteristic of the corresponding OFDM-IM subblock. This is reasonable because OFDM subblocks have distinct levels of robustness against noise. However, the amplitude constraint in the recent work is efficient for only additive white Gaussian noise (AWGN) channels and cannot be used for maximum likelihood (ML) detection. Therefore, in this paper, based on pairwise error probability (PEP) analysis, a specific constraint for the dither signals is derived over a Rayleigh fading channel.

key words: *index modulation (IM), orthogonal frequency division multiplexing (OFDM), peak-to-average power ratio (PAPR)*

1. Introduction

Orthogonal frequency division multiplexing with index modulation (OFDM-IM) [1] is an emerging technique which is the application of the spatial modulation (SM) [2] principle to the subcarriers in an OFDM system [3]. In OFDM-IM, the subcarriers are partitioned into many subblocks and the subcarriers in each subblock have two states, active or idle. Then, OFDM-IM conveys information through both modulated symbols and the indices of the active subcarriers. For the same spectral efficiency, OFDM-IM is widely known to have a superior bit error rate (BER) performance, compared to the classical OFDM [1]. Also, OFDM-IM systems have a better energy efficiency compared to the classical OFDM [4]. Therefore, OFDM-IM is receiving a lot of attention [5], [6].

The authors in [7] pointed out that OFDM-IM inherits the high peak-to-average power ratio (PAPR) problem from the classical OFDM. It is known that the high PAPR induces in-band distortion and out-of-band radiation in consideration of nonlinear high power amplifier (HPA). Numerous PAPR reduction schemes have been researched for decades such as selected mapping (SLM), partial transmit sequence (PTS), and tone injection (TI) [8]. Recently, there is a method to reduce PAPR by taking advantage of the degrees of freedom provided by cyclic prefix or guard subcarriers in an OFDM structure [9]. To solve the high PAPR problem in OFDM-IM, we may borrow the PAPR reduction schemes designed for the classical OFDM. However, those methods are not efficient because they do not consider the unique characteristic of OFDM-IM structure. Specifically, they do not exploit the idle subcarriers in OFDM-IM.

Therefore, the authors in [10] proposed a PAPR reduction method using the idle subcarriers in OFDM-IM. In specific, the scheme in [10] introduces dither signals in the idle subcarriers for reducing PAPR of OFDM-IM signals. This is the first PAPR reduction method exploiting the special structure of OFDM-IM. This methodology is quite reasonable because the dither signals in the idle subcarriers do not considerably affect the error performance in high signal-to-noise ratio (SNR) region. This is because the symbol error event with diversity order of one dominates the system performance in the high SNR region and the dither signals cannot affect this error event. To suppress the harmful effect of the dither signals, they also proposed the equivalent amplitude constraint for the dither signals.

Meanwhile, in the same time, the authors in [11] proposed a PAPR reduction method, where the dither signals in idle subcarriers are generated by clipping procedure. Their methodology is similar to the scheme in [10] except that there are no amplitude constraints for the dither signals. Due to the harmful effect of the dither signals, its BER performance is significantly degraded especially if the clipping ratio is small.

The recent work dealing with dither signals in idle subcarriers in [12] considered the fact that the amplitude characteristics of the subblocks are distinct when quadrature amplitude modulation (QAM) is employed in the active subcarriers. Therefore, a variable amplitude constraint for dither signals is proposed. As a result, the constraint in [12] gives the dither signals more freedom in average while maintaining good demodulation performance. However, in [12], the amplitude constraint is derived under the assumption of an additive white Gaussian noise (AWGN) channel without fading. Also, the low complexity power based detection algorithm is considered in the derivation. Unfortunately, the power based detection is less preferred in the recent literature

Manuscript received June 30, 2023.
Manuscript revised October 3, 2023.
Manuscript publicized January 30, 2024.

[†]The author is with the School of Electronic and Electrical Engineering, Hankyong National University, Anseong 17579, South Korea.

*There is an arXiv preprint (https://arxiv.org/abs/2205.13793).

a) E-mail: keehk85@gmail.com

DOI: 10.23919/transcom.2023EBP3110

because of its degraded performance (in the recent literature [13]–[15], it is known that the optimal maximum likelihood (ML) detector can be implemented with low complexity). Therefore, the derivation of the amplitude constraint in [12] is not efficient for a fading channel and the receiver with ML detector. Also, there is a work dealing with dither signals in [16] exploiting the channel knowledge at the transmitter, which is a rare case in mobile communications. Note that the proposed scheme and the works in [10], [11], and [12] do not use channel knowledge at the transmitter.

In this paper, based on rigorous pairwise error probability (PEP) analysis, a new amplitude constraint for the dither signals is proposed for the ML detector over a Rayleigh fading channel, which is more complicated than that considered in the previous work. Therefore, it is remarkable that the derivation in this paper is completely different from the previous work in [12]. By using the proposed amplitude constraint, PAPR reduction dither signals can be well designed in OFDM-IM systems over a fading channel.

2. System Model

2.1 OFDM-IM

Consider an OFDM-IM system with N subcarriers and total m information bits. These m information bits are divided into g subblocks, where each subblock conveys p bits, i.e., $m = pg$. Also, the p bits in each subblock are mapped to one subblock of length n in the frequency domain, where $n = N/g$. The specific mapping procedure is that only k out of n subcarriers in each subblock are activated, where the subcarrier activation pattern (SAP) is determined by the first p_1 bits of the p bits. Then, the M-ary modulated symbols on the k active subcarriers are determined by the remaining $p_2 = k \log_2 M$ bits of the p bits, i.e., $p = p_1 + p_2$. Of course, the idle subcarriers have zero values in the frequency domain [1].

We denote the set of the indices of the k active subcarriers in the β-th OFDM-IM subblock, $\beta = 0, 1, \cdots, g-1$, as

$$I^\beta = \{i_0^\beta, i_1^\beta, \cdots, i_{k-1}^\beta\}$$

with $i_\gamma^\beta \in \{0, 1, \cdots, n-1\}$ for $\gamma = 0, 1, \cdots, k-1$. Also, we denote the set of k modulated symbols as

$$S^\beta = \{S_0^\beta, S_1^\beta, \cdots, S_{k-1}^\beta\},$$

where $S_\gamma^\beta \in \mathcal{S}$ and $\mathcal{S}$ is the M-ary signal constellation.

By considering I^β and S^β, the β-th OFDM-IM subblock in frequency domain can be generated as

$$X^\beta = [X_0^\beta \; X_1^\beta \; \cdots \; X_{n-1}^\beta]^T,$$

where X_i^β is the i-th element of X^β and $i = 0, 1, \cdots, n-1$. After all of the g subblocks $\{X^\beta\}_{\beta=0}^{g-1}$ are generated, they are concatenated into the symbol sequence $\mathbf{X}$ of length N in frequency domain. To achieve the frequency diversity gain as much as possible, concatenation in an interleaved pattern is generally employed [17]. By the interleaved pattern, the elements in an OFDM-IM subblock can experience independent fading channels.

Then, to obtain the OFDM-IM signal sequence $\mathbf{x}$ in time domain, the symbol sequence $\mathbf{X}$ in frequency domain is processed by the inverse discrete Fourier transform (IDFT) as

$$\mathbf{x} = \mathrm{IDFT}(\mathbf{X}).$$

Figure 1 summarises the transmission procedure of OFDM-IM signals.

For transmission, cyclic prefix (CP) insertion and digital-to-analog (D/A) conversion are sequentially performed and then the PAPR of the resultant continuous-time OFDM-IM signal $x(t)$ is defined by

$$\mathrm{PAPR}(x(t)) = \frac{\max_t |x(t)|^2}{\mathbb{E}[|x(t)|^2]}.$$

Practically, to capture PAPR of the continuous-time OFDM-IM signal, four-times oversampling of $\mathbf{x}$ is used.

The receiver firstly detects the SAP, called index demodulation in this paper, and demodulates the M-ary modulated symbols in the active subcarriers. There have been several detection algorithms for OFDM-IM systems [1], [18]. For low computational complexity, a power based detection algorithm can be employed, but it degrades the error performance of OFDM-IM.

For β-th OFDM-IM subblock, optimal ML detection can be described as

$$\{\hat{I}^\beta, \hat{S}^\beta\} = \arg\min_{\tilde{I}, \tilde{S}} \sum_{i=1}^{n} |Y_i^\beta - H_i^\beta X_i^\beta|^2, \tag{1}$$

where Y_i^β and H_i^β are the i-th element of β-th received OFDM-IM subblock and the corresponding channel frequency response, respectively. Also, $\tilde{I}$ and $\tilde{S}$ are feasible SAP and modulated symbols, respectively. Note that its complexity is too huge to implement.

Fortunately, in [13]–[15], it is known that the optimal ML detection can be implemented with low complexity and thus it is preferred to employ the ML detection. Therefore, different from the previous work in [12] considering the power based detector, the derivation in this paper considers the ML detector at the receiver.

3. PAPR Reduction Using Dither Signals

3.1 PAPR Reduction Using Dither Signals of an Equivalent Amplitude Constraint [10]

In OFDM-IM, there are two types of error events, an index demodulation error event and a symbol error event [19]. The former is the error event when the SAP is incorrectly detected and the latter is the error event when the modulated symbols

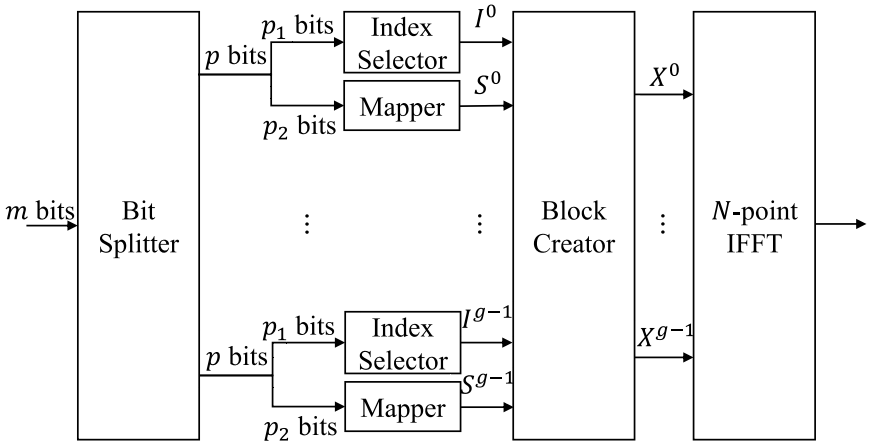

Fig. 1 A block diagram of the OFDM-IM system.

in the active subcarriers are incorrectly detected though the SAP is correctly detected. As described in [1], the symbol error event has the diversity order of one and the index demodulation error event has the diversity order of two. By virtue of the frequency diversity gain, the index demodulation error event occurs less frequently than the symbol error event in high SNR region. That is, the symbol error event dominates the overall error performance of the OFDM-IM system in high SNR region. Therefore, in [10] there is an attempt to reduce PAPR by inserting the dither signals in the idle subcarriers. Clearly, this dither signal does not affect the symbol error event and only degrades the index demodulation error performance. Also, the authors in [10] introduces an equivalent amplitude constraint for the dither signals in the idle subcarriers.

Specifically, the dither signal added in the β-th OFDM-IM subblock is

$$D^{\beta} = [D_0^{\beta}\ D_1^{\beta}\ \cdots\ D_{n-1}^{\beta}]^T$$

and the constraint in [10] with a hyperparameter R is

$$D_i^{\beta} = \begin{cases} |D_i^{\beta}| < R, & i \in (I^{\beta})^c \\ 0, & i \in I^{\beta} \end{cases}, \tag{2}$$

where $(I^{\beta})^c$ is the complement set of I^{β}, i.e., indices of the idle subcarriers. Then, $X^{\beta}+D^{\beta}$ becomes a new β-th OFDM-IM subblock with dither signals. Under the constraint in (2), the values of D^{β} are determined in order to reduce PAPR of $x(t)$. In [10], convex programming is used, but iterative clipping and filtering with trimming can be alternatively used.

Specifically, the iterative clipping and filtering with trimming is a slight modification of the well known clipping and filtering in [20]. First, the symbol sequence $\mathbf{X}$ with zero padding is first transformed using an $4N$ point IDFT. This results in trigonometric interpolation (or oversampling) of $\mathbf{x}$. The interpolated signal is then clipped. The clipping is followed by filtering to reduce out-of-band radiation. The filter consists of two discrete Fourier transform (DFT) operations. The forward DFT transforms the clipped signal back into the frequency domain. Then the in-band components are trimmed in order to obey the constraint in (2) and then passed to the inputs of the second IDFT while the out-of-band components are nulled. The above procedure may be iteratively done several times to reduce much PAPR.

Note that the decoding procedure in (1) is not changed. This simplicity at the receiver side is the advantage of using dither signals.

3.2 PAPR Reduction with Dither Signals of a Variable Amplitude Constraint [12]

Meanwhile, in [12], a variable amplitude constraint for dither signals is proposed. This is motivated from the fact that the OFDM-IM subblocks have different robustness against channel noise if higher modulation than 16-QAM is employed. Using this, the amplitude constraint of dither signals can be varied for subblocks. Let us briefly review the work in [12].

First, for the β-th OFDM-IM subblock X^{β}, we define A^{β} as

$$A^{\beta} = \min(|S_0^{\beta}|, |S_1^{\beta}|, \cdots, |S_{k-1}^{\beta}|).$$

For ease of understanding, we assume that 16-QAM is employed with the signal constellation $\{\pm 1 \pm j1, \pm 1 \pm j3, \pm 3 \pm j1, \pm 3 \pm j3\}$ from now on (clearly, the scheme in [12] can also be easily described for higher modulations such as 64-QAM or 256-QAM). Then, A^{β} can be one of $\{\sqrt{2}, \sqrt{10}, \sqrt{18}\}$.

Second, assuming an AWGN channel with noise power N_0, the PEP for the β-th subblock is

$$P(X^{\beta} \to \hat{X}^{\beta}) = P(X \to \hat{X}) = Q\left(\frac{\|X - \hat{X}\|}{\sqrt{2N_0}}\right), \tag{3}$$

where, without loss of generality, we omit β for simplicity and $\hat{X} = [\hat{X}_0\ \hat{X}_1\ \cdots\ \hat{X}_{n-1}]^T$. Also, $Q(\cdot)$ means the Q-function, the tail distribution function of the standard normal distribution. It is clear that the PEP in (3) depends on the Euclidean distance between X and $\hat{X}$, $\|X - \hat{X}\|$.

Third, we focus on the index demodulation error event

because the dither signals do not affect the symbol error event as we mentioned. Then, the fundamental index demodulation error in the β-th subblock is the case when the u-th subcarrier is detected as active and the v-th subcarrier is detected as idle when actually the opposite is true. The shortest Euclidean distance inducing this fundamental index demodulation error is

$$\min \sqrt{|\hat{X}_u|^2 + |X_v|^2} = \sqrt{2 + (A^\beta)^2},$$

where the index demodulation error performance of the β-th subblock is dominated by this metric. That is, as A^β becomes larger, the robustness of the β-th OFDM-IM subblock against the index demodulation error increases. Therefore, dither signals with large amplitude may be inserted if A^β is large.

Using these three facts, in [12], the dither signals can have different amplitudes according to A^β as

$$D_i^\beta = \begin{cases} |D_i^\beta| < R_0, & i \in (I^\beta)^c \text{ and } A^\beta = \sqrt{2} \\ |D_i^\beta| < R_1, & i \in (I^\beta)^c \text{ and } A^\beta = \sqrt{10} \\ |D_i^\beta| < R_2, & i \in (I^\beta)^c \text{ and } A^\beta = \sqrt{18} \\ 0, & i \in I^\beta. \end{cases}$$

Also, the constraint proposed in [12] is

$$\sqrt{2} - R_0 = \sqrt{10} - R_1 = \sqrt{18} - R_2, \tag{4}$$

where the power based detection algorithm at the receiver is considered.

Since PEP in (3) assumes an AWGN channel and the constraint in (4) is derived for the power based detector, the constraint in (4) is not efficient for the ML detector and fading channels, as we described earlier. One example of the possible candidates is $R_0 = 0.2$, $R_1 \simeq 1.9$, and $R_2 \simeq 3$, which is efficient over an AWGN channel. However, this candidate is inappropriate for frequency selective fading channels because the high values of R_1 and R_2 induce the index demodulation error event inevitably.

4. Proposed Dither Signals Design over a Rayleigh Fading Channel

In this section, we propose an amplitude constraint of the dither signals with consideration of a Rayleigh fading channel. First, we denote the channel frequency response (CFR) of the i-th element in the β-th OFDM-IM subblock as H_i (with omission of β) and the CFR matrix is denoted as $H = \mathrm{diag}(H_0, H_1, \cdots, H_{n-1})$. Note that $H_0, H_1, \cdots, H_{n-1}$ are approximately independent because we use concatenation in an interleaved pattern (this is a valid assumption unless we use channels with less than n taps in time domain). For a given matrix H, the conditional PEP of the β-th OFDM-IM subblock with the dither signal D is

$$\begin{aligned} &P(X + D \to \hat{X}|H) \\ &= P(\|Y - H\hat{X}\|^2 < \|Y - HX\|^2|H) \\ &= P(\|H(X + D) + Z - H\hat{X}\|^2 < \|HD + Z\|^2|H) \\ &= P(2 \cdot \mathrm{Re}\{(HD + Z)^H H(X - \hat{X})\} \\ &\quad < -\|H(X - \hat{X})\|^2|H), \end{aligned} \tag{5}$$

where $Y = H(X + D) + Z$ is the β-th received OFDM-IM subblock and Z is AWGN with $Z_i \sim \mathcal{CN}(0, N_0)$.

Since the dither signals cannot affect the symbol error events, let us consider the fundamental index demodulation error case that the u-th subcarrier is detected as active and the v-th subcarrier is detected as idle when actually the opposite is true. That is, $X_u = 0, \hat{X}_u \neq 0$ and $X_v \neq 0, \hat{X}_v = 0$ in (5). Also, $X_i = \hat{X}_i$ when $i \neq u$ and $i \neq v$.

Then, (5) becomes

$$\begin{aligned} &P(X + D \to \hat{X}|H) \\ &= P(\mathrm{Re}\{-|H_u|^2 D_u^* \hat{X}_u - H_u Z_u^* \hat{X}_u + H_v Z_v^* X_v\} \\ &\quad < -\frac{1}{2}(|H_u \hat{X}_u|^2 + |H_v X_v|^2)|H), \end{aligned} \tag{6}$$

where D_u is the dither signal in the u-th idle subcarrier in X. If we consider the dither signal D_u satisfying

$$|\mathrm{Re}\{D_u\}| + |\mathrm{Im}\{D_u\}| = \sqrt{2}R$$

then the left hand side (LHS) term in (6) becomes

$$-R|H_u|^2|\hat{X}_u| + \mathrm{Re}\{-H_u Z_u^* \hat{X}_u + H_v Z_v^* X_v\} \tag{7}$$

under the assumption of $|\mathrm{Re}\{\hat{X}_u\}| = |\mathrm{Im}\{\hat{X}_u\}|$ and $\hat{X}_u$ and D_u lie on the same quadrant (this assumption is valid because we are considering the weakness case inducing the index demodulation error. Specifically, $X_u = 0$ and the nearest signal point among the possible candidates of $\hat{X}_u$ from $X_u = 0$ is $\hat{X}_u = \pm 1 \pm j1$ for all modulations). Clearly, (7) is Gaussian distributed as

$$\mathcal{N}(-R|H_u|^2|\hat{X}_u|, \frac{N_0}{2}(|H_u \hat{X}_u|^2 + |H_v X_v|^2)).$$

Then, (6) becomes

$$\begin{aligned} &P(X + D \to \hat{X}|H) \\ &= Q\left(\frac{|H_u \hat{X}_u|^2 + |H_v X_v|^2 - 2R|H_u|^2|\hat{X}_u|}{\sqrt{2N_0}\sqrt{|H_u \hat{X}_u|^2 + |H_v X_v|^2}}\right) \\ &= Q\left(\frac{1}{\sqrt{2N_0}}\left(\sqrt{|H_u \hat{X}_u|^2 + |H_v X_v|^2}\right.\right. \\ &\quad \left.\left. - \frac{2R|H_u||H_u \hat{X}_u|}{\sqrt{|H_u \hat{X}_u|^2 + |H_v X_v|^2}}\right)\right), \end{aligned} \tag{8}$$

where the term $\sqrt{|H_u \hat{X}_u|^2 + |H_v X_v|^2} - \frac{2R|H_u||H_u \hat{X}_u|}{\sqrt{|H_u \hat{X}_u|^2 + |H_v X_v|^2}}$ in (8) can be depicted as the red line in Fig. 2.

As seen in Fig. 2, the length of the red line can be alternatively approximated as the length of the green line. The reason is that the difference between the green and red lines in Fig. 2, $2R|H_u| \sin\theta$, mainly depends on $|H_u|$ and the error event $X + D \to \hat{X}$ usually occurs when $|H_u| \ll 1$.

The length of the green line is

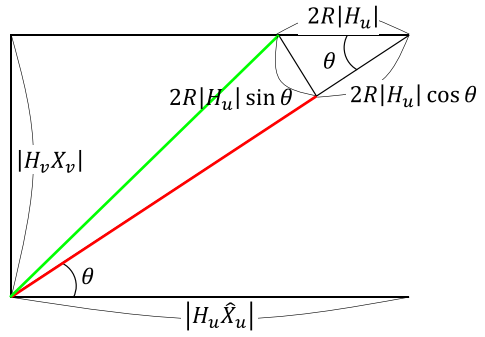

Fig. 2 A geometrical representation of $\sqrt{|H_u\hat{X}_u|^2+|H_vX_v|^2} - \frac{2R|H_u||H_u\hat{X}_u|}{\sqrt{|H_u\hat{X}_u|^2+|H_vX_v|^2}}$ by the led line. Note that $\frac{|H_u\hat{X}_u|}{\sqrt{|H_u\hat{X}_u|^2+|H_vX_v|^2}}$ is $\cos\theta$.

$$\sqrt{|H_u(|\hat{X}_u|-2R)|^2+|H_vX_v|^2}$$

in Fig. 2 and thus (8) becomes

$$P(X+D\to\hat{X}|H) \simeq Q\left(\frac{\sqrt{|H_u(|\hat{X}_u|-2R)|^2+|H_vX_v|^2}}{\sqrt{2N_0}}\right). \quad (9)$$

Meanwhile, it is known that the unconditional PEP with independent Rayleigh channel frequency responses $H_i \sim \mathcal{CN}(0,1)$ in high SNR region is expressed as [21], [22]

$$\begin{aligned} P(X\to\hat{X}) &= \int P(X\to\hat{X}|H)p(H)dH \\ &= \int Q\left(\frac{\|H(X-\hat{X})\|}{\sqrt{2N_0}}\right)p(H)dH \\ &\simeq \frac{(4N_0)^{\Gamma_{X,\hat{X}}}}{2\Pi_{i\in\mathcal{G}_{X,\hat{X}}}\eta_i}, \end{aligned} \quad (10)$$

where $p(H)$ is the probability distribution function (pdf) of H, η_i is the i-th element of $|X-\hat{X}|^2$, $\mathcal{G}_{X,\hat{X}}=\{i|\eta_i\neq 0\}$, and $\Gamma_{X,\hat{X}}=|\mathcal{G}_{X,\hat{X}}|$. By combining (9) and (10), we have

$$P(X+D\to\hat{X}) \simeq \frac{(4N_0)^2}{2(|\hat{X}_u|-2R)^2\cdot|X_v|^2}.$$

That is, the unconditional PEP $P(X+D\to\hat{X})$ depends on the metric as

$$(|\hat{X}_u|-2R)\cdot|X_v|.$$

Then, the weakness case inducing the fundamental index demodulation error in the β-th subblock depends on the metric as

$$\min(|\hat{X}_u|-2R)\cdot|X_v| = (\sqrt{2}-2R)\cdot A^\beta. \quad (11)$$

Clearly, the index demodulation error performance of the β-th OFDM-IM subblock is dominated by the value of (11).

As in the scheme in [12], the proposed scheme is valid if QAM modulation is considered. If 16-QAM is employed with the signal constellation $\{\pm1\pm j1,\pm1\pm j3,\pm3\pm j1,\pm3\pm j3\}$, the proposed variable amplitude constraint is shown in (12) at the top of the next page.

In (12), the values of R_0, R_1, and R_2 are determined by

$$(\sqrt{2}-2R_0)\cdot\sqrt{2} = (\sqrt{2}-2R_1)\cdot\sqrt{10} = (\sqrt{2}-2R_2)\cdot\sqrt{18}, \quad (13)$$

which leads to the same value of (11) for all subblocks (since the bottleneck of the OFDM-IM error performance relates to the smallest value of (11) for all g subblocks, this strategy could be the optimal solution). It is straightforward to generate the constraints for other modulations.

Table 1 shows several examples of the values of R_0, R_1, and R_2 satisfying the proposed amplitude constraint in (13). We remark that the values of R_1 and R_2 are suppressed because of frequency selective fading channels, compared to the values from (4).

Table 1 Examples of R_0, R_1, and R_2 values satisfying (13).

R_0	R_1	R_2
0.1	0.435	0.504
0.2	0.480	0.538
0.3	0.525	0.571
0.4	0.569	0.604
0.5	0.614	0.638

The benefit of the proposed constraint over the equivalent amplitude constraint comes from the increased freedom of dither signals in the subblocks having $A^\beta=\sqrt{10}$ or $\sqrt{18}$. Therefore, it is clear that the proposed scheme gives a better benefit as $n-k$ decreases.

5. Simulation Results

Here we provide the simulation results of OFDM-IM signals with various amplitude constraints. For modulating the symbols in the active subcarriers, 16-QAM is used. Also, we use $N=128$, $n=4$, and $k=2$. The OFDM-IM subblocks are concatenated in an interleaved pattern and dither signals are generated by five times iterative clipping and filtering with trimming for all schemes. The clipping ratio is 5 dB. The only difference of tested schemes is amplitude constraints for the dither signals. Therefore, the computational complexities of the tested schemes are same. To capture PAPR of the continuous-time OFDM-IM signal, four-times oversampling is used for the clipping and filtering. At the receiver, the optimal ML detection with low computational complexity is employed. Also, we consider a Rayleigh fading channel with eight channel taps.

We do not consider the traditional PAPR reduction schemes such as SLM, PTS, and TI in [8] because they do not exploit the idle subcarriers in OFDM-IM (recently, the authors in [23] proposed a SLM scheme for non-coherent OFDM-IM. But, the non-coherent OFDM-IM system is out of scope).

Figure 3 shows the PAPR reduction performance of the

$$D_i^\beta = \begin{cases} |\mathrm{Re}\{D_i^\beta\}| + |\mathrm{Im}\{D_i^\beta\}| < \sqrt{2}R_0, & i \in (I^\beta)^c,\ A^\beta = \sqrt{2} \\ |\mathrm{Re}\{D_i^\beta\}| + |\mathrm{Im}\{D_i^\beta\}| < \sqrt{2}R_1, & i \in (I^\beta)^c,\ A^\beta = \sqrt{10} \\ |\mathrm{Re}\{D_i^\beta\}| + |\mathrm{Im}\{D_i^\beta\}| < \sqrt{2}R_2, & i \in (I^\beta)^c,\ A^\beta = \sqrt{18} \\ 0, & i \in I^\beta \end{cases} \tag{12}$$

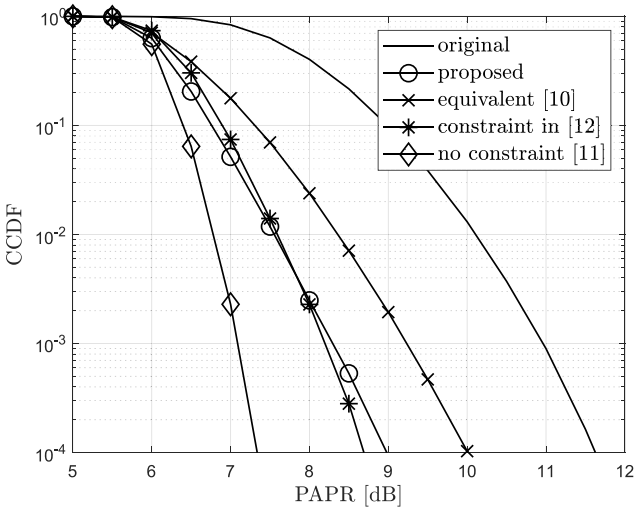

Fig. 3 PAPR reduction performance of the OFDM-IM signals with different amplitude constraints. Four-times oversampling is used.

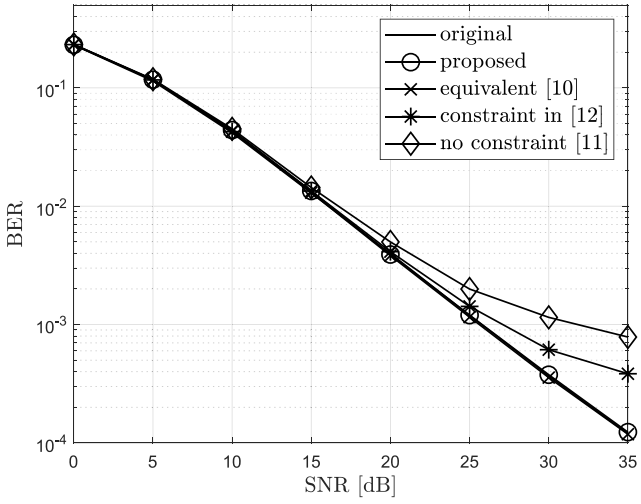

Fig. 4 BER performance of the OFDM-IM signals with different amplitude constraints. SSPA with 5 dB is considered.

five cases. The meaning of five labels in the legend is as follows:

1. Original OFDM-IM signals without clipping.
2. OFDM-IM signals under the proposed amplitude constraint, $R_0 = 0.3$, $R_1 = 0.525$, and $R_2 = 0.571$.
3. OFDM-IM signals under the equivalent amplitude constraint in [10], $R = 0.3$.
4. OFDM-IM signals under the constraint in [12], $R_0 = 0.2$, $R_1 = 0.7$, and $R_2 = 1.718$, which is originally designed for AWGN channels.
5. OFDM-IM signals with no constraint in [11].

In Fig. 3, the ordinate is the complementary cumulative distribution function (CCDF) of the PAPR. The case of no constraint shows the best PAPR reduction performance because we do not trim the dither signals after the clipping in this case. However, it is inevitable that the non-trimmed dither signals give harmful effect to BER performance, which will be shown. Using the proposed amplitude constraint can reduce much PAPR than the scheme in [10] using the equivalent amplitude constraint. This result mainly comes from the fact that the proposed constraint provides a larger freedom to the dither signals compared to the scheme in [10].

Figure 4 and Fig. 5 show the BER performance and the power spectral density (PSD) of OFDM-IM signals, respectively. Here, we consider passing the OFDM-IM signal through a solid-state power amplifier (SSPA) with limited linear range. The input/output relationship of SSPA can be written as $y(t) = \frac{|x(t)|}{\left(1+\left(\frac{|x(t)|}{C}\right)^{2p}\right)^{\frac{1}{2p}}} e^{j\phi(t)}$ where $x(t) = |x(t)|e^{j\phi(t)}$ is the normalized input, and $y(t)$ is the output of SSPA [24]. We use $p = 3$ and $C = 5$ dB here.

In Fig. 4, the SNR means the average energy per bit over N_0. For fair comparison, both symbols in the active subcarriers and dither signals in the idle subcarriers are considered when we calculate the average energy per bit (that is, for a fixed SNR point, the schemes using dither signals allocate less power to information bits compared to the original OFDM-IM).

The proposed constraint and the equivalent amplitude constraint in [10] have almost the same BER performance because the two constraints induce the same PEP for the bottleneck of the OFDM-IM error performance. In specific, they have the same smallest value of (11) for all g subblocks. However, the constraint $R_0 = 0.2$, $R_1 = 0.7$, and $R_2 = 1.718$ originally designed for AWGN channels in [12] shows the error floor over 25 dB SNR point because the large values of R_1 and R_2 induce the index demodulation error event inevitably over a fading channel. Also, no constraint case clearly shows the error floor over 25 dB SNR point because the harmful effect of dither signals is not suppressed.

In Fig. 5, the proposed constraint shows less out-of-band radiation than that of the equivalent amplitude constraint, which can also be induced from Fig. 3.

To sum it up, the proposed constraint shows the almost

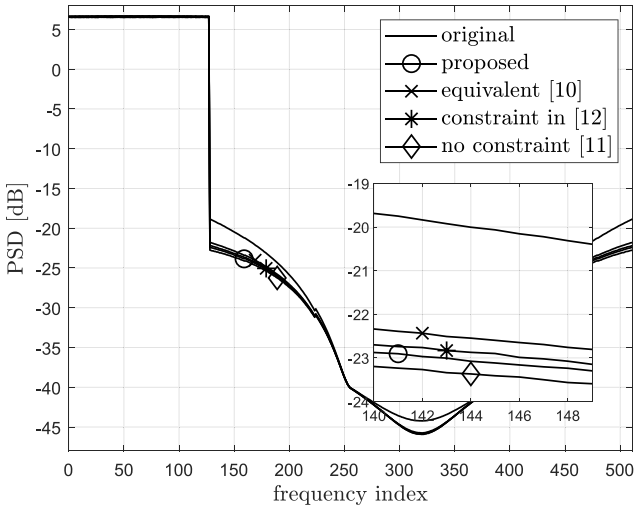

Fig. 5 PSD of the OFDM-IM signals with different amplitude constraints. Four-times oversampling is used to invest out-of-band radiation. SSPA with 5 dB is considered.

same BER performance and better PAPR reduction performance (or less out-of-band radiation in PSD) compared to the equivalent amplitude constraint in [10]. Also, the constraint by the previous work [12] and the no constraint case in [11] show the poor BER performance over a fading channel because they are not carefully designed for fading channels and give harmful effect to pairwise error events.

6. Conclusion

In this paper, we derived the amplitude constraint for the PAPR reduction dither signals in OFDM-IM systems over a Rayleigh fading channel. In consideration with the ML detector at the receiver, the derivation is based on the rigorous PEP analysis. By using the proposed amplitude constraint, the PAPR reduction performance can be maximized without degradation of BER performance.

References

[1] E. Başar, Ü. Aygölü, E. Panayırcı, and H.V. Poor, "Orthogonal frequency division multiplexing with index modulation," IEEE Trans. Signal Process., vol.61, no.22, pp.5536–5549, 2013.
[2] R. Mesleh, H. Haas, S. Sinanovic, C.W. Ahn, and S. Yun, "Spatial modulation," IEEE Trans. Veh. Technol., vol.57, no.4, pp.2228–2241, 2008.
[3] S. Sugiura, T. Ishihara, and M. Nakao, "State-of-the-art design of index modulation in the space, time, and frequency domains: Benefits and fundamental limitations," IEEE Access, vol.5, pp.21774–21790, 2017.
[4] L. Zhao, H. Zhao, K. Zheng, and Y. Yang, "A high energy efficient scheme with selecting sub-carriers modulation in OFDM system," 2012 IEEE International Conference on Communications (ICC), pp.5711–5715, 2012.
[5] D. Kim, H. Lee, and J. Kang, "Accurate error probability analysis of MCIK-OFDM with a low-complexity detection over TWDP fading channels," IEICE Trans. Commun., vol.E101-B, no.6, pp.1347–1351, June 2018.
[6] Q. Wang, G. Dou, R. Deng, and J. Gao, "Linear constellation precoded OFDM with index modulation based orthogonal cooperative system," IEICE Trans. Commun., vol.E103-B, no.4, pp.312–320, April 2020.
[7] N. Ishikawa, S. Sugiura, and L. Hanzo, "Subcarrier-index modulation aided OFDM-will it work?," IEEE Access, vol.4, pp.2580–2593, 2016.
[8] S.H. Han and J.H. Lee, "An overview of peak-to-average power ratio reduction techniques for multicarrier transmission," IEEE Wireless Commun., vol.12, no.2, pp.56–65, 2005.
[9] S. Liu, Y. Wang, Z. Lian, Y. Su, and Z. Xie, "Joint suppression of PAPR and OOB radiation for OFDM systems," IEEE Trans. Broadcast., vol.69, no.2, pp.528–537, 2023.
[10] J. Zheng and H. Lv, "Peak-to-average power ratio reduction in OFDM index modulation through convex programming," IEEE Commun. Lett., vol.21, no.7, pp.1505–1508, 2017.
[11] E. Memisoglu, E. Basar, and H. Arslan, "Low complexity peak-to-average power ratio reduction in OFDM-IM," 2018 IEEE International Black Sea Conference on Communications and Networking (BlackSeaCom), pp.1–5, IEEE, 2018.
[12] K.H. Kim, "PAPR reduction in OFDM-IM using multilevel dither signals," IEEE Commun. Lett., vol.23, no.2, pp.258–261, 2019.
[13] B. Zheng, F. Chen, M. Wen, F. Ji, H. Yu, and Y. Liu, "Low-complexity ML detector and performance analysis for OFDM with in-phase/quadrature index modulation," IEEE Commun. Lett., vol.19, no.11, pp.1893–1896, 2015.
[14] X. Zhang, H. Bie, Q. Ye, C. Lei, and X. Tang, "Dual-mode index modulation aided OFDM with constellation power allocation and low-complexity detector design," IEEE Access, vol.5, pp.23871–23880, 2017.
[15] Z. Hu, S. Lin, B. Zheng, F. Chen, Q. Wang, and Y. Wei, "Low-complexity subcarrier-wise detection for MIMO-OFDM with index modulation," IEEE Access, vol.5, pp.23822–23832, 2017.
[16] S. Watanabe, T. Miyajima, and Y. Sugitani, "Dither signal design for PAPR reduction in OFDM-IM," IEICE Proceedings Series, vol.57, no.RS2-1, pp.98–103, 2019.
[17] Y. Xiao, S. Wang, L. Dan, X. Lei, P. Yang, and W. Xiang, "OFDM with interleaved subcarrier-index modulation," IEEE Commun. Lett., vol.18, no.8, pp.1447–1450, 2014.
[18] A.I. Siddiq, "Low complexity OFDM-IM detector by encoding all possible subcarrier activation patterns," IEEE Commun. Lett., vol.20, no.3, pp.446–449, 2016.
[19] Y. Shi, X. Lu, K. Gao, J. Zhu, and S. Wang, "Subblocks set design aided orthogonal frequency division multiplexing with all index modulation," IEEE Access, vol.7, pp.52659–52668, 2019.
[20] J. Armstrong, "Peak-to-average power reduction for OFDM by repeated clipping and frequency domain filtering," Electron. Lett., vol.38, no.5, pp.246–247, 2002.
[21] M.K. Simon and M.S. Alouini, Digital Communication over Fading Channels, John Wiley & Sons, 2005.
[22] T. Van Luong and Y. Ko, "Spread OFDM-IM with precoding matrix and low-complexity detection designs," IEEE Trans. Veh. Technol., vol.67, no.12, pp.11619–11626, 2018.
[23] S. Gopi and S. Kalyani, "An optimized SLM for PAPR reduction in non-coherent OFDM-IM," IEEE Wireless Commun. Lett., vol.9, no.7, pp.967–971, 2020.
[24] R. van Nee and R. Prasad, OFDM for Wireless Multimedia Communications, Artech House, 2000.

Kee-Hoon Kim received the B.S., M.S., and Ph.D. degrees in electrical engineering and computer science from Seoul National University, Seoul, Korea, in 2008, 2010, and 2015, respectively. He was a Senior Engineer at Samsung Electronics from 2015 to 2017. He was an Assistant Professor in the Department of Electronic Engineering at Soonchunhyang University from 2017 to 2020. He is currently an Assistant Professor in the School of Electronic and Electrical Engineering at Hankyoung National University, Korea. His area of research interests includes compressed sensing, OFDM systems, and communication theory.